

Construction Optimization and Application of Shield Launching Reaction Frame of Large Diameter Shield Tunnel

*Zhuang Xie, **Jinyang Fu*, ***Junsheng Yang, ****Yufeng Shi, *****Wenhua Guo

* School of Civil Engineering, Central South University,
Changsha 410075, China, (249814997@qq.com)

** School of Civil Engineering, Central South University,
Changsha 410075, China, (jyfu2010@163.com)

*** School of Civil Engineering, Central South University,
Changsha 410075, China, (jsyang@csu.edu.cn)

**** School of Civil Engineering and Architecture Dept, East China Jiaotong University,
Nanchang 330013, China (s074811156@126.com)

***** School of Civil Engineering, Central South University,
Changsha 410075, China, (whguo@126.com)

Abstract

The reaction force of shield launching usually comes from the main structure behind the launching shaft. Due to special reasons, however, the main structure behind the launching shaft sometimes fails to provide a fulcrum to the upper structure of the reaction frame. In this case, the optimization plans should be sought for. In light of the delay in completing the middle plate of the main structure behind the launching shaft in a large diameter shield tunnel, this paper, aiming at ensuring the scheduled launching of the shield tunneling machine, proposes an optimization plan that moves the fulcrum of the reaction force from the middle plate to the bottom plate via inclined supports, and analyzes and evaluates the safety of the reaction frame optimization plan for shield launching through the combination of numerical simulation and field measurement. The results show that the reaction frame has small horizontal and vertical displacements during shield launching, and the support strength and reaction frame stability fall within the allowable range. Therefore, the proposed reaction frame satisfies the engineering safety requirements. Moreover, the numerical calculation results are echoed by the results of field measurement. The

optimization plan proposed in this paper is simple and reliable, and sheds new light on the design and installation of shield launching reaction frame of shield tunnel in the future.

Key words

Shield tunnel, Reaction frame, Stress test, Numerical simulation

1. Introduction

As an advanced tunnel construction technology, the shield method has become the mainstream approach to construct cross-river tunnels thanks to its unique advantages. [1-4] The shield launching is of critical importance to the entire project because it is the make-or-break phase of the shield tunneling. Overshadowed by extremely high construction risks, this phase brings more difficulties to the control of the attitude of the shield tunneling machine and the ground subsidence than the normal stage. [5-8] Against this backdrop, Engineers are much concerned about whether the support strength and overall stability of the reaction frame, the source of the reaction force for shield launching, meet the safety requirements.

In view of the above issue, the following research has been carried out by industrial experts. For instance, Zhao Baohu et al. put forward a field monitoring plan based on the numerical calculation of the stress distribution of the shield launching reaction frame in Wuhan Yangtze River Tunnel, analyzed the load distribution and changes of the reaction frame during shield launching in light of measured data, and thereby provided the source data for reaction frame strength analysis and optimization design in shield tunneling. [9] Whereas it is impossible to deploy reaction frame in the vertical shafts of the tunnels crossing the Yellow River, Fu Zhiyuan et al. succeeded in the plan to transform the vertical shaft wall into a load bearing reaction pedestal that provides the launching reaction force for the shield tunneling machine. [10] Wu Yanxia designed the structure of shield launching reaction frame (steel ring, main beam, supports and embedded parts), performed finite element calculation and analysis, and applied the design to several metro construction projects. It is proved in the analysis and applications that the reaction frame has sufficient strength and stiffness to provide the reaction force for the launch of the shield tunneling machine. [11]

The research object of this paper is the Xiangjiang River Tunnel on Nanhu Road, Changsha, China. The large diameter shield tunnel ($\phi 11.65\text{m}$) is affected by the delay in land acquisition and resettlement. The middle plate of the main structure behind the launching shaft has not been completed as planned, resulting in the lack of the fulcrum to the upper structure of the reaction frame. To ensure the scheduled launch of the shield tunneling machine, this paper prepares an

optimization plan to alter the horizontal supports of shield launching reaction frame into inclined supports, thus moving the fulcrum of the reaction force from the middle plate to the bottom plate. Besides, it employs FLAC3D finite element software to calculate the axial force and stress of the inclined supports, and preliminarily demonstrates the feasibility of the inclined supports plan. In addition, this paper presents a stress and displacement monitoring plan for the shield launching phase, aiming at monitoring the whole process from shield launching to the removal of temporary segments in real time. The monitoring results are used to evaluate the safety of the optimized reaction frame. This is the first time for any Chinese scholar to optimize the shield launching reaction frame of large diameter shield tunnel with inclined supports. The proposed plan opens a new way for the design of shield launching reaction frame.

2. Overview of Reaction Frame Design

The Xiangjiang River Tunnel on Nanhu Road is the first highway tunnel in Hunan Province that is constructed with the shield tunneling machine. It is constructed by French-made NFM composite slurry-balanced shield tunneling machine. The main line is designed at a speed of 50km/h. The northern line, a 1,374.9m-long shield tunnel, was completed early on March 3rd, 2013. After installation and commissioning, the shield tunneling machine was launched integrally for test run at a slope of 4% on December 26th, 2011.

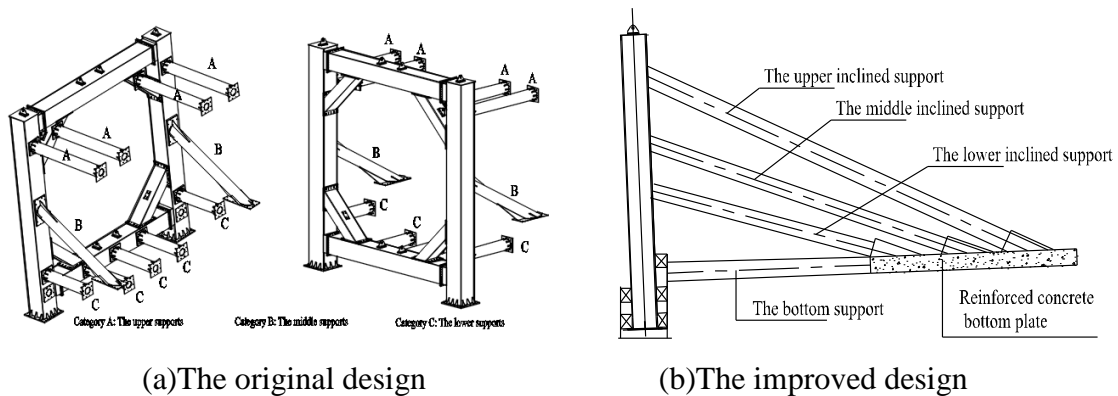


Fig.1. The structure of the reaction frame

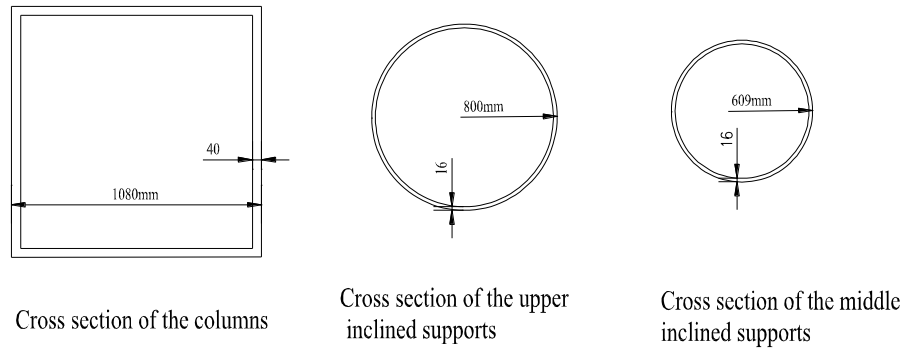


Fig.2. Sectional views of the components of the reaction frame

The reaction frame is a symmetrical structure consisting of a door frame and a number of supports. On one side, the frame is connected to the contact ring on the tunnel lining to receive the thrust transmitted by the jack. On the other side, the frame is connected to the rear fixed structure via a number of supports to withstand the thrust of shield launching. The supports are generally divided into horizontal supports in the upper parts, the inclined supports in the middle parts, and the horizontal supports in the lower parts. (Figure 1-a) Due to the delay in the construction of the main structure behind the launching shaft, there is no fulcrum of reaction force for the upper horizontal supports in this project. Hence, the author plans to optimize the original support plan into a structure of 6 eudipleural inclined supports and 5 horizontal supports at the bottom, where the upper, middle and lower inclined supports deviate from the columns of the reaction frame by an angle of 73° , 69° and 63° , respectively. (Figure 1-b) The columns and beams of the reaction frame are hollow square section pipes made of 1,080mm×40mm (width×thickness) steel plates. Each pipe is made up of 4 steel plates. The upper inclined supports are $\Phi 800$ mm, $t = 16$ mm steel pipes, while the middle and lower inclined supports are $\Phi 609$ mm, $t = 16$ mm steel pipes. The 5 horizontal supports at the bottom are concrete supports (Figure 2).

The inclined support plan mainly faces two problems: (1) Local shear and punch failures may occur on the inclined supports and the bottom pedestal under the action of the horizontal component force; (2) The reaction frame and the columns might move up under the action of the vertical force.

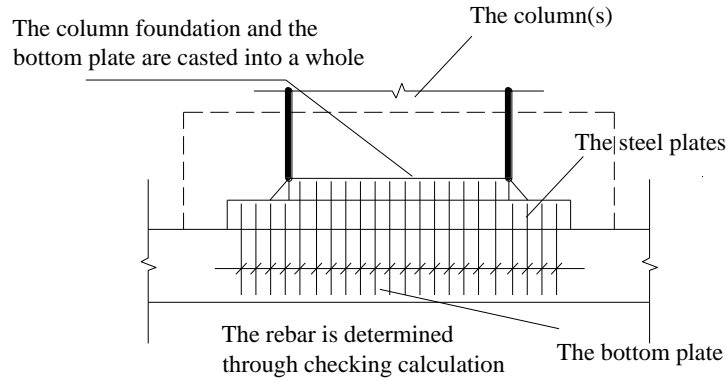


Fig.3. The column foundation

Facing these problems, the optimization plan adopts the following local reinforcement measures: (1) Create an overall bearing structure by embedding rebar in the bottom plate of the main structure and weld the rebar firmly to the rebar of the pedestal; (2) Prevent the reaction frame from moving upward by embedding hollow square section steel plates in the bottom plate below the lower beam of the reaction frame and tie the steel plates to the pedestal and beams of the reaction frame; Plus, strengthen the pulling resistance of the columns by pouring the column foundation and the bottom plate into a whole (Figure 3).

3. Numerical simulation of reaction frame safety

In consideration of the pulling resistance and shear strength of the columns, the foundation, the inclined supports and the bottom pedestal, the optimization plan adopts local strengthening measures. Since this is not enough to maintain the overall safety of the optimization plan, the author makes further analysis of reaction frame safety by FLAC^{3D} numerical calculation software.

3.1 Simplification and establishment of the model

The model is simplified for the numerical analysis (Figure 4). The reaction frame and the supports are simulated by beam elements, the bottom plate is simulated by solid element, which is linear elastic material, and the lower soil is simulated by solid element, which follows the Mohr-Coulomb yield criterion. The boundary conditions are: (x) is the horizontal constraint, (y) is the longitudinal displacement constraint, (z) is the vertical restraint, and the upper surface is free. The structure elements abide by the following boundary conditions: the beams are rigidly connected to the columns; the lower ends of the columns are fixed to the foundation and the top

ends are free. The inclined supports are rigidly connected to the reaction frame via the same node, and fixed to the bottom plate. The horizontal supports at the bottom are rigidly connected to the reaction frame, and the tension rod of the lower beam is rigidly connected to the beam; the rod is fixed to the floor.

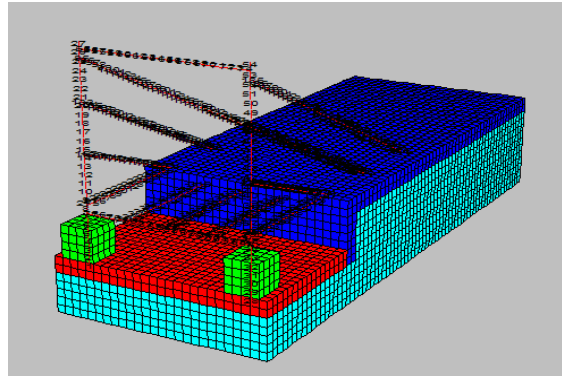


Fig.4. The simplified model for numerical simulation

The worst working condition is considered in the calculation (the first tunnel ring). The geometrical and physical properties of the structural elements are shown in Table 1 below, while the parameters of the stratum and reinforced concrete floor are shown in Table 2.

Tab.1. Geometrical and physical parameters of the reaction frame and inclined supports

Name of structural element	Density (kg/m ³)	Elastic modulus /GPa	Poisson's ratio	Sectional area/m ²	Moment of inertia/m ⁴	Polar moment of inertia/m ⁴
Columns and beams	7800	210	0.2	0.1664	0.03	0.06
Upper inclined supports	7800	210	0.2	0.0394	0.00303	0.00606
Middle and lower inclined supports	7800	210	0.2	0.0298	0.00131	0.00262
Bottom supports	7800	210	0.2	0.0298	0.00131	0.00262

Tab.2. Physical parameters of solid elements

Name of element	Density kg/m ³	Elastic modulus/Pa	Poisson's ratio	Cohesion/kpa	Frictional angle/°
Reinforced concrete bottom plate	2400	32e9	0.2	—	—
Stratum	1900	100e6	0.35	100	30

2.2 Determination and simplification of shield launching thrust

The shield launching thrust is simplified into a 3,000T (lower than 3,000T in actual launching) uniform force on the beam element node. Due to the 4% descent at shield launching,

there is a 4% angle between the thrust and the horizontal direction. Figure 5 displays the simplified mechanical model of the shield launching thrust.

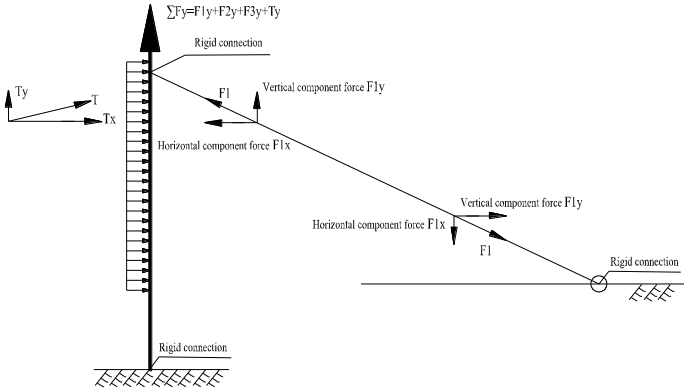


Fig.5. The mechanical model of the shield launching thrust

4. Analysis of numerical simulation results

4.1 Axial force and stress of inclined supports

Under the 3,000T launching thrust, the axial force and the corresponding stress of each support of the reaction frame is as shown in Table 3.

Tab.3. Axial force and the corresponding stress of each support

Name	Upper inclined supports	Middle inclined supports	Lower inclined supports
Axial force/KN	5068	2962	1851
Stress/MPa	128.6	99.4	62.1

According to the results of numerical calculation, under the action of 3,000T thrust, the upper inclined supports have the largest axial force, followed by the middle-inclined supports, while the lower inclined supports have the smallest axial force. The stress of each of the 6 supports is smaller than 180.8Mpa, the allowable stress of the Q235 steel (the safety factor is 1.3), which satisfies the strength requirements on steel supports.

4.2 Reaction frame deformation

The 3,000T thrust causes a certain amount of deformation to the reaction frame. (Figure 6) The most obvious deformation is about 32mm, which appears at the upper beam and tends to move upward. The columns and the lower beam have very slight deformation, which is between 5mm and 8mm. The significant horizontal deformation of the upper beam is caused by the

simplification of the model. Since the model does not take the C beam into account, the actual deformation must be less than the calculation results, and should be determined by construction monitoring.

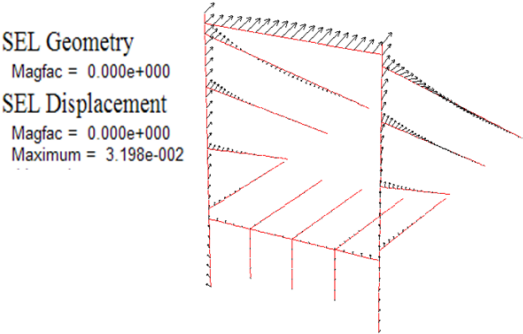


Fig.6. Vector graph of reaction frame deformation

5. Field displacement and axial force monitoring of the reaction frame

5.1 Monitoring plan

(1) Reaction frame displacement

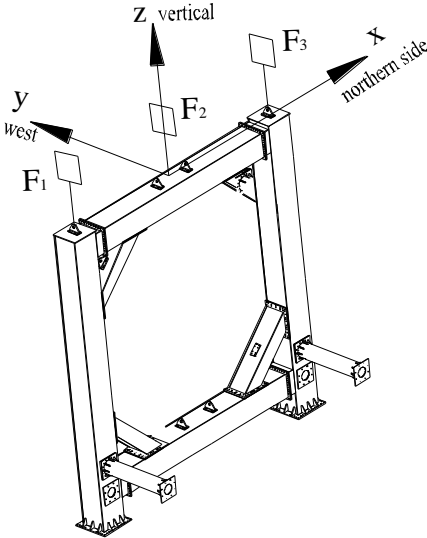


Fig.7. Arrangement of displacement monitoring points

The three displacement monitoring points (F1, F2 and F3) are arranged respectively at the top of the two columns and the middle of the upper beam. (Figure 7) The horizontal and vertical displacements of the reaction frame are obtained through real-time monitoring of the horizontal and vertical displacements of the measuring points of F1, F2 and F3.

(2) The axial force of inclined supports of the reaction frame

A pair of surface-mounted 350Ω temperature self-compensating resistance strain gauges is placed on each of the 6 inclined supports, which are distributed symmetrically on the north and south sides. The measuring points are arranged as shown in Figure 8. The surface strain of the steel supports is monitored in real time, and the surface stress of each inclined support is obtained on the basis of the strain. The axial force of the inclined supports are calculated by simplifying the structure into a combined bending bearing components.

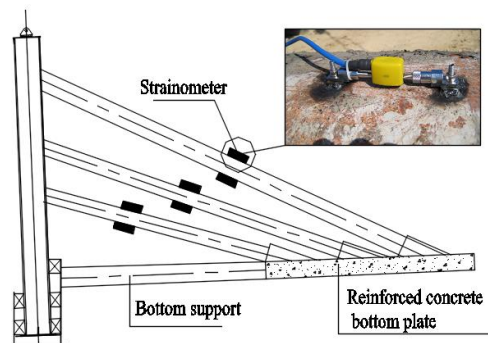


Fig.8. The arrangement of the axial force measuring points on the supports

5.2 Analysis and discussion of monitoring results

The actual thrust of the shield tunneling machine is 1,500T. When the machine excavates to the 30th ring, the thrust reaches 4,000T. (Figure 9) At this time, part of the thrust is balanced by the friction between the lining ring and the surrounding rock wall. After calculating the magnitude of the fracture, it is found that the actual thrust on the reaction frame is smaller than 3,000T.

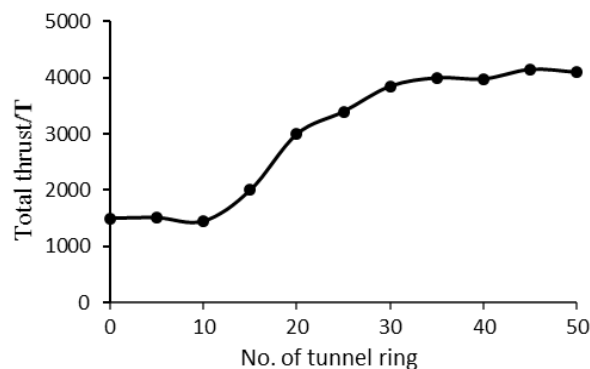


Fig.9. The thrust of jack of different excavation distances

(1) Displacement monitoring

The author carries out a three-month-long real-time field monitoring of the displacement and stress from the 1st tunnel ring at the launching to the 50th tunnel ring, and removes the reaction frame and the 51st tunnel ring. According to the deformation monitoring results of the reaction frame, the y-direction deformation at all measuring points increases gradually at the beginning of the excavation. However, after the tunnel has been excavated to a certain distance, the deformation of each measuring point gradually declines towards the stable value (3~5mm).

Tab.4. The maximum displacement of the reaction frame (mm)

Measuring point	Horizontal displacement		Vertical displacement
	x	y	z
F1	-2.30	-11.15	2.3
F2	-5.25	-8.15	-
F3	3.85	-17.50	1.8

Note: Positive value indicates that the direction is the same with the coordinate axis, and negative value indicates the opposite.

Table 4 lists the maximum displacement of the measuring points. It can be seen that the reaction frame moves up slightly (by about 2mm), which is basically negligible. In the shield launching phase, the reaction frame suffers a certain amount of deformation laterally (the x-direction). The deformation is small (5mm at the maximum), but subjected to direction changes. This indicates that the force transmitted from the jack of the shield tunneling machine to the reaction frame is loaded unsymmetrically during the shield launching phase. Comparatively speaking, the reaction frame has a larger displacement in the direction opposite to the shield launching (the y-direction), which is maximized at 17.5mm. The displacements of the left and right columns are largely the same, with very minor differences.

The above monitoring results show that the deformation of the reaction frame is very small and tends to be stable. Hence, the optimized plan can meet the stability requirements of the shield launching reaction frame.

(2) Stress monitoring

During the excavation of the shield tunneling machine, the axial force of the supports of the reaction frame changes with the thrust and the number of tunnel rings. Figure 10 shows how the axial force of the northern and southern supports change with the tunnel rings (The lower inclined support on the northern side is damaged).

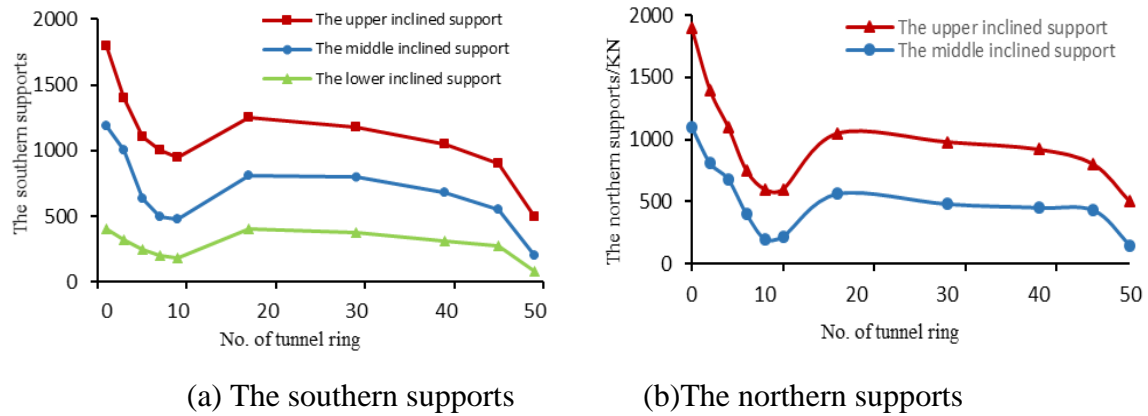


Fig.10. The relationship between the axial forces of the supports and the tunnel rings

It can be inferred from Figure 10 that the axial force of each support is higher in shield launching than other phases. The upper inclined supports boast the largest axial force, which is about 1,800-1,900kN; the axial force of each support changes in the following manner: increase, decline, stabilize, decline and level off; In each of the three pairs, the northern side support has basically the same axial force with the southern side support. Among the three inclined supports on each side, the upper support has the largest axial force, followed by the middle support, and the lower support has the smallest axial force.

The load bearing conditions of the inclined supports are well demonstrated by the field monitoring. The axial force of each support is changed as follows: decrease, increase, stabilize and decline. When the shield tunneling machine starts to operate, the thrust is entirely applied to the reaction support. As the excavation continues, the thrust is partially balanced by the friction between the partial segments and the surrounding rock, and the axial force of the reaction frame gradually declines. After reaching the 10th tunnel ring, the thrust rockets up, and so it is with the axial force of the reaction frame. Between the 20th ring and the 45th ring, the axial force of the reaction frame is relatively stable because the increase in thrust is almost the same with the increase in the amount of thrust balanced by the external friction of the partial segments. Passing the 45th ring, the axial force of the reaction frame begins to fall slowly because the friction between the partial segments and the surrounding rocks continues to rise as the thrust no longer increases. When it comes to the 50th ring, the axial force of the reaction frame stabilizes and remains on a low level because the reaction force required for excavation is largely provided by the friction between the partial segments and the surrounding rocks. In this case, the reaction frame can be removed.

The above monitoring results show that the upper inclined supports have the highest axial force, which is about 1,900kN; the corresponding stress is 48.2Mpa, much smaller than the allowable stress of Q235 steel. Therefore, the optimized reaction frame satisfies the requirements on shield launching strength.

(3) Comparison with the numerical calculation results

1) The author carries out a preliminary numerical calculation of the support strength and reaction frame stability and a targeted monitoring of the construction process. The results of the two methods are highly consistent: both meet the safety requirements of shield launching. Meanwhile, the monitoring results verify the reliability of the numerical calculation.

2) The thrust of numerical calculation is twice the magnitude of the actual thrust (the first tunnel ring). Under this condition, both the support strength and reaction frame stability fulfil the safety requirements. The optimization plan is very conservative, leaving a space for further improvement. In actual construction, one can step up the progress by properly increasing the shield launching thrust in light of the monitoring results.

6. Conclusion

Targeted at the Xiangjiang River Tunnel on Nanhu Road, a large diameter shield tunnel, this paper puts forward a plan to optimize the reaction frame to handle the absence of the fulcrum of reaction force caused by the delay in completing the middle plate of the main structure behind the launching shaft. Through numerical simulation and analysis and field monitoring, it is revealed that the stress and deformation are within the allowable range, indicating that the optimization plan features simplicity, reliability and desirable application effect.

This paper discovers that there is some surplus in the support strength and stability of the reaction frame. In view of the monitoring results, the shield launching thrust should be properly adjusted in actual construction to optimize the construction plan without sacrificing the safety. With inclined supports, the proposed reaction frame structure provides support and reaction force for shield excavation, and resolves the delay in actual construction of the main structure behind the launching shaft in an effective manner. Nevertheless, the unsymmetrical loading should be avoided during the excavation. The successful application of the proposed reaction frame, which is characterized by the inclined supports, provides a valuable reference for similar projects.

References

1. S. Okubo, K. Fukui, W. Chen, Expert system for applicability of tunnel boring machines in Japan, 2003, *Rock Mechanics and Rock Engineering*, vol. 36, no. 4, pp. 305-322.
2. J. Buchanan, Review of developments in full-face tunnel boring machines for rock, 1987, *Mining Engineer*, vol. 147, no. 314, pp. 189-192, 194.
3. K. Naitoh, Development of earth pressure balanced shields in Japan, 1985, *Tunnels and Tunneling*, vol. 17, no. 5, pp. 15-18.
4. P. Yurkevich, Developments in Segmental Concrete Lining for Subway Tunnels in Belarus, 1995, *Tunneling and Underground Space Technology*, vol. 10, no. 3, pp. 353-355.
5. K. Chen, K.R. Hong, X.S. Wu, *Shield Construction Technique*, 2010, Beijing China Communications Press.
6. F. Wei., Originating technique for the shield-driven tunnel, 2006, *Sci-Tech Information Development & Economy*, no. 2.
7. G. Li, H.W. Huang, Risk ansysis on arriving into shaft of super large diameter shield machine underwater, 2009, *Chinese Journal of Underground Space & Engineering*, no. 5, pp. 1423-1426.
8. B.Y. Zhang, The key technology of super large diameter shield tunnel, 2013, *Journal of Underground Space and Engineering*, vol. 9, no. 3, pp. 633-639.
9. B.H. Zhao, Y.Q. Wang, C. Yue, Y. Kang, H. Wang, Stress Monitoring and Safety Evaluation of the Counter force Frame during Shield Originating, 2009, *Engineering Mechanics*, vol. 26, no. 9, pp. 105-111.
10. Z.Y. Fu, C. Zhang, Design of new type of reaction abutment of working shaft in northern bank of tunnel crossing Yellow River, 2011, *Yangtze River*, vol. 42, no. 8, pp. 41-46.
11. Y.X. Wu, Design and application of the reaction frame for shield tunneling, 2009, *Road Machinery & Construction Mechanization*, vol. 26, no. 2, pp. 64-66.